

Formation of spinel structured compounds in the lithium permanganate thermal decomposition

Alexander A. Andriiko · Arseniy Ye. Shpak ·
Yuriy O. Andriyko · José R. García ·
Sergei A. Khainakov · Nataliya Ye. Vlasenko

Received: 12 August 2011 / Revised: 13 November 2011 / Accepted: 18 November 2011 / Published online: 3 December 2011
© Springer-Verlag 2011

Abstract Products of thermal decomposition of lithium permanganate $\text{LiMnO}_4 \cdot 3\text{H}_2\text{O}$, which are formed in temperature range 160–900 °C, have been characterized by powder XRD and chemical analysis. It has been found that the decomposition of the permanganate results in the formation of an equimolar mixture of manganate(IV) Li_2MnO_3 and stoichiometric spinel LiMn_2O_4 at the temperatures above 700 °C. Intermediate products with spinel structure are formed at lower temperatures with oxidation number of manganese being between +4 and +3.5. These compounds can be related to *overstoichiometric* spinel phases with general formula $\text{Li}_a[\text{Mn}_{(1+0.5a)}\text{Li}_{(1-0.5a)}]\text{O}_4$, where $a > 1$. Electrochemical properties of these intermediates with regard to the reaction of Li extraction were investigated. The data are of interest for the development of synthesis methods for mixed oxides containing lithium and manganese with lithium permanganate as the lithiating reagent.

Keywords Lithium permanganate · Thermal decomposition · Overstoichiometric spinels · Electrochemical properties

Introduction

Oxide compounds of the Li–Mn–O system are of considerable interest for application as active materials in lithium electrochemical cells [1, 2]. Such oxides can conveniently be divided in two types—“3 V” and “4 V”, depending on their behavior in electrochemical cells with Li metal electrodes. Some compositions of Li_2O – MnO_2 [3–6] system, orthorhombic LiMnO_2 [7–10], and *overstoichiometric* spinel $\text{Li}_{1+x}\text{Mn}_2\text{O}_4$ [11, 12] belong to the first type.

Stoichiometric spinel LiMn_2O_4 , which was studied in the large number of papers [13–16], is probably the most interesting “4 V” oxide for Li-ion battery applications. Some compounds formed inside the composition triangle $\lambda\text{-MnO}_2$ – $\text{Li}_4\text{Mn}_5\text{O}_{12}$ – Mn_3O_4 of the Li–Mn–O system with distorted spinel structure are also of “4 V” type [17]. Other known compounds of the Li–Mn–O system, manganate(IV) Li_2MnO_3 with rock salt structure [18], are electrochemically inactive [19].

Lithium permanganate $\text{LiMnO}_4 \cdot 3\text{H}_2\text{O}$ is stable in the presence of water molecules in the crystal lattice and decomposes on attempt to remove this water. It is a useful precursor for synthesis of various complex oxide compounds containing Li, Mn, and other transition metals [3, 6]. For example, the rechargeable 3V oxides of Li_2O – MnO_2 system were easily prepared by the reaction of lithium permanganate with manganese dioxide [6]. We investigated thermal decomposition of this compound in order to estab-

A. A. Andriiko (✉) · A. Y. Shpak · N. Y. Vlasenko
Chair of General and Inorganic Chemistry, Chemical Technology
Faculty, National Technical University of Ukraine “KPI”,
Prospekt Peremogy 37,
03056 Kyiv, Ukraine
e-mail: Andriiko_aa@ukr.net

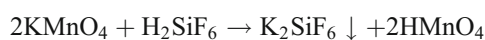
Y. O. Andriyko
CEST—Centre of Electrochemical Surface Technology,
Viktor Kaplan-Strasse 2,
2700 Wiener Neustadt, Austria

J. R. García · S. A. Khainakov
Departamento de Química Orgánica e Inorgánica,
Universidad de Oviedo—CINN,
33006 Oviedo, Spain

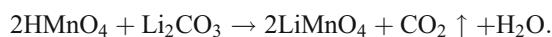
lish the main reaction products (both final and intermediate) and check their electrochemical behavior in Li cells. Such data are of practical importance for the development of synthesis routes for preparation of Mn-based oxide materials for electrochemical applications.

Experimental

Lithium permanganate trihydrate is not commercially available. That is why it was prepared from chemically pure-grade potassium permanganate KMnO_4 (Macrochem, Ukraine) and lithium carbonate Li_2CO_3 (Merck). The synthesis was performed in two steps. First, solution of permanganate acid was prepared by the reaction of potassium permanganate with hexafluorosilicic acid:



This solution was neutralized by lithium carbonate:

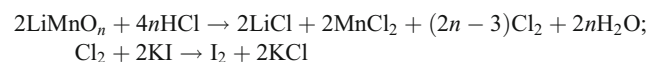


The resulting solution was concentrated by evaporation, cooled down to 8–10 °C on ice; the crystals of $\text{LiMnO}_4 \cdot 3\text{H}_2\text{O}$ were filtered and dried in ambient air. Thus prepared, the product has an assay of 96%, which was established by chemical titrimetric method (reaction with HCl) similar to that described below.

Thermal decomposition of lithium permanganate was investigated by in situ powder XRD analysis using an X'Pert PRO MPD X-ray diffractometer with PIXcel detector, operating in the Bragg-Brentano ($\theta/2\theta$) geometry, and using $\text{CuK}\alpha$ radiation ($\lambda=1.5418 \text{ \AA}$). The initial sample was preliminary heated in an alumina crucible at 250 °C for 1.5 h and then placed into the diffractometer. The diffractograms were obtained from 300 to 850 °C with 50 °C step (heating rate between measurements was 5 °C/min, relaxation time before measurement 15 min). Data were collected over the angular 2θ range 10–90°, with a step size of 0.0131°.

The samples for chemical analysis were prepared by heating of the crystals of lithium permanganate in alumina crucibles at chosen temperatures for 1.5 h and cooling down to the room temperature. Some of these samples were also investigated by powder XRD with a DRON-3M diffractometer ($\text{CuK}\alpha$ radiation).

Chemical analysis of the samples was carried out. This analysis consists in dissolution of the specimen in concentrated hydrochloric acid in presence of potassium iodide according to the reactions:



with subsequent titration of the formed iodine by sodium thiosulfate solution. Thus, the quantity of liberated iodine is

equivalent to the change in the oxidation state of Mn, which permits to calculate the overall content of oxygen in the sample using the equation

$$n = \frac{61.9\nu + 1.5m}{m - 16\nu},$$

where m is the mass of the sample for analysis (in milligrams), ν is the amount of liberated iodine (in millimoles), which is calculated from the volume of the titrant (in milliliters) and its concentration (in moles/liter). The error of such determination does not exceed 0.002 units of n in the formula LiMnO_n .

Quantity of Li, which could be reversibly extracted from the structure of sample, was established in electrochemical experiments, which were performed in Li/EC to DMC+1 M LiPF_6 /sample mockup button cell of the 2016 dimension. The cells were assembled in argon filled dry glove box. Positive electrode was prepared by slurring the testing material (85 wt.%) with KS6 graphite (10 wt.%) and PVDF as a binder in *N*-methyl-pyrrolidone and pasting the slurry onto the thin aluminum foil. Testing of the cells was performed by PC-governed multichannel equipment in both galvanostatic and linear sweep voltammetry conditions.

Results and discussion

According to DTA, lithium permanganate trihydrate crystals begin to decompose at 130–140 °C with evolution of water and oxygen just after melting. The reaction is highly exothermic and should be carried out carefully to avoid sputtering.

We have studied the products of decomposition obtained at several temperatures in air. Table 1 represents the overall chemical compositions of the samples according to the chemical analysis. Fig. 1 shows the in situ powder XRD patterns of the samples. Following the data, structure of the samples obtained at the temperatures below 700 °C corresponds to cubic spinel ($Fd\bar{3}m$), which becomes to form at about 160 °C.

The weak diffraction peaks corresponding to the Li_2MnO_3 phase appear at 650 °C (they are marked by asterisks in Fig. 1). The intensity of these reflections gradually increases since 700 to 800 °C and does not change at 850 °C. Thus, the samples obtained at 800 °C and higher temperatures contains two phases: lithium manganate(IV) Li_2MnO_3 and stoichiometric spinel LiMn_2O_4 .

We have calculated the lattice constant of the cubic spinel phase from the powder XRD data (Fig. 2). As follows from these data, the lattice parameter tends to increase when the decomposition temperature increases, though this tendency is not smooth.

Evidently, the size of the lattice unit should be related to the chemical composition of the sample. In order to observe

Table 1 Chemical and phase composition of the $\text{LiMnO}_4 \cdot 3\text{H}_2\text{O}$ decomposition products at different temperatures

Temperature (°C)	Mn average oxidation number	Spinel notation	Phase composition
200	3.742	$\text{Li}_{1.374}[\text{Mn}_{1.687}\text{Li}_{0.313}]\text{O}_4$	Overstoichiometric spinel (OS)
250	3.742	$\text{Li}_{1.374}[\text{Mn}_{1.687}\text{Li}_{0.313}]\text{O}_4$	
300	3.728	$\text{Li}_{1.384}[\text{Mn}_{1.692}\text{Li}_{0.308}]\text{O}_4$	
350	3.736	$\text{Li}_{1.378}[\text{Mn}_{1.689}\text{Li}_{0.311}]\text{O}_4$	
400	3.754	$\text{Li}_{1.366}[\text{Mn}_{1.683}\text{Li}_{0.317}]\text{O}_4$	
450	3.762	$\text{Li}_{1.360}[\text{Mn}_{1.680}\text{Li}_{0.320}]\text{O}_4$	
500	3.778	$\text{Li}_{1.348}[\text{Mn}_{1.674}\text{Li}_{0.326}]\text{O}_4$	
550	3.768	$\text{Li}_{1.356}[\text{Mn}_{1.678}\text{Li}_{0.322}]\text{O}_4$	
600	3.748	$\text{Li}_{1.370}[\text{Mn}_{1.685}\text{Li}_{0.315}]\text{O}_4$	
650	3.738	$\text{Li}_{1.376}[\text{Mn}_{1.688}\text{Li}_{0.312}]\text{O}_4$	
700	3.702	$\text{Li}_{1.402}[\text{Mn}_{1.701}\text{Li}_{0.299}]\text{O}_4$	OS+ Li_2MnO_3
750	3.694	$\text{Li}_{1.408}[\text{Mn}_{1.704}\text{Li}_{0.296}]\text{O}_4$	OS+ Li_2MnO_3
800	3.672		$\text{LiMn}_2\text{O}_4 + \text{Li}_2\text{MnO}_3$
850			

this relationship, the values of the lattice constant must be corrected for the thermal expansion of the lattice. For that, we used the experimental data on the relative increase of the a -parameter in form of the linear correlation shown in Fig. 3.

After the correction on the thermal expansion, the dependency of the lattice constant on the decomposition temperature (Fig. 4) shows minimum at 500 °C, which coincides with the maximum of oxygen content in the sample according to the chemical analysis (Fig. 4). Except for the two initial (300 and 350 °C) and one final (800 °C) temperatures, very good correlation is observed between the lattice constant and oxygen content.

To explain the obtained data, we assume the formation of the spinel structured compounds of general formula $\text{Li}_m[\text{Li}_{2-b}\text{Mn}_b]\text{O}_4$ ($m=(2b-2)>1$), with Mn atoms

being in the octahedral positions and Li being distributed between the tetrahedral and octahedral sites. The formulas of these compounds in the spinel notation are given in the third column of Table 1. Since the number of Li atoms in the tetrahedral sites $m>1$, we should denote these compounds as *overstoichiometric* spinels, in contrast to the *normal* spinels AB_2O_4 with one atom A in the tetrahedral positions of the spinel formula.

It is clear that the lattice must shrink when the larger Mn atoms in the octahedral sites are replaced with smaller Li atoms. Thus, one should expect the correlation between the lattice constant and the number of Mn atoms in the spinel formula. Such linear correlation is really good for the samples formed in the temperature range from 500 to 750 °C (Fig. 5), which belong to the descending of the oxygen content (Fig. 4, curve 2) while ascending the cell parameter

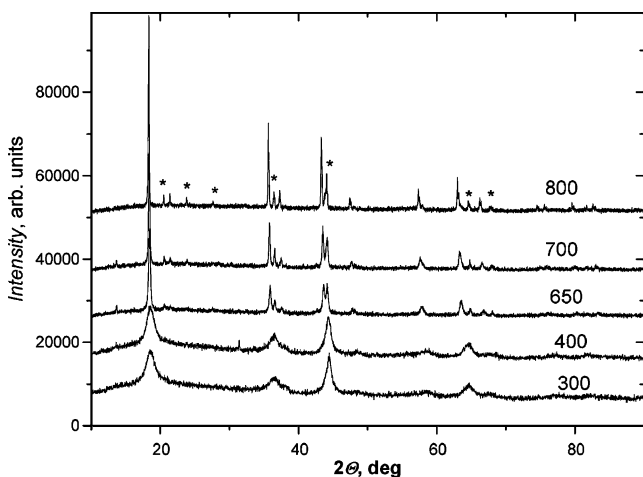


Fig. 1 Powder XRD patterns for $\text{LiMnO}_4 \cdot 3\text{H}_2\text{O}$ obtained in situ at different temperatures (see Table 1). The peaks corresponding to the Li_2MnO_3 phase are marked with asterisks

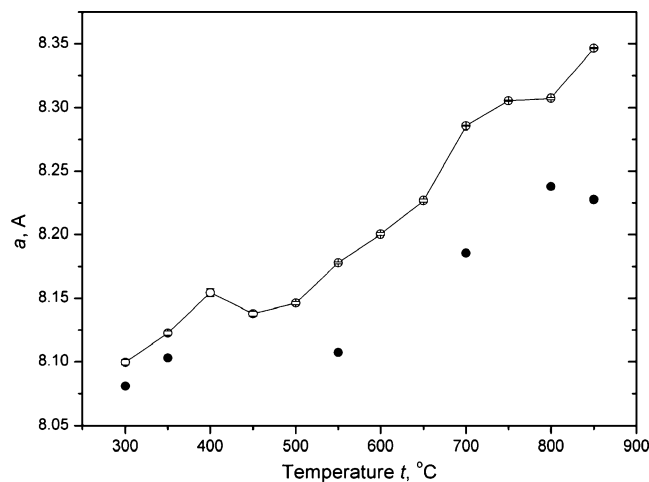


Fig. 2 Variation of the lattice constant of the cubic spinel phase with the decomposition temperature. *Open circles* in situ measurements, *filled circles* at 25 °C

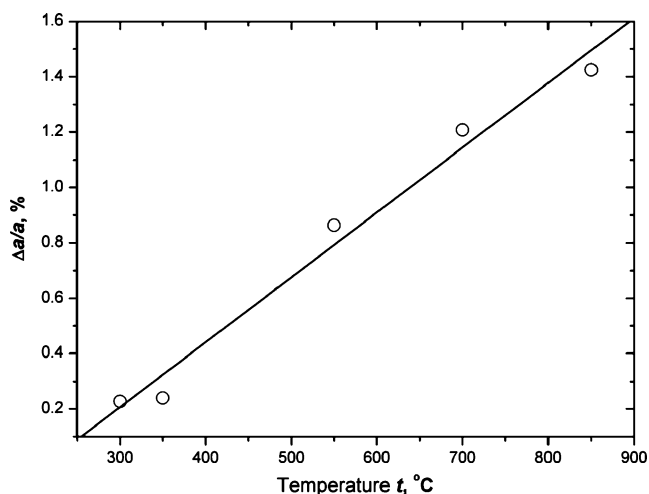
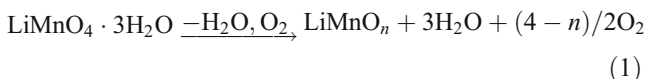


Fig. 3 Linear thermal expansion of the lattice vs. temperature obtained from the data of Fig. 2

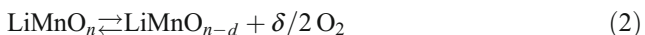
(Fig. 4, curve 1). The sample obtained at 800 °C, which is related to two-phase mixture and does not represent the *oversoichiometric* spinel, drops out of the correlation.

Thus, the formation of the spinel phases occurs at the temperatures near 150–200 °C by the reaction



where the product LiMnO_n in the spinel notation can be represented as $\text{Li}_{\frac{8}{n}-2} \left[\text{Mn}_{\frac{4}{n}} \text{Li}_{2-\frac{4}{n}} \right] \text{O}_4$.

Further on, the product loses oxygen:



This results in the increase of the number of Mn atoms in the octahedral positions and decrease of their average oxidation state. Since the effective ionic radius of Mn^{3+} is

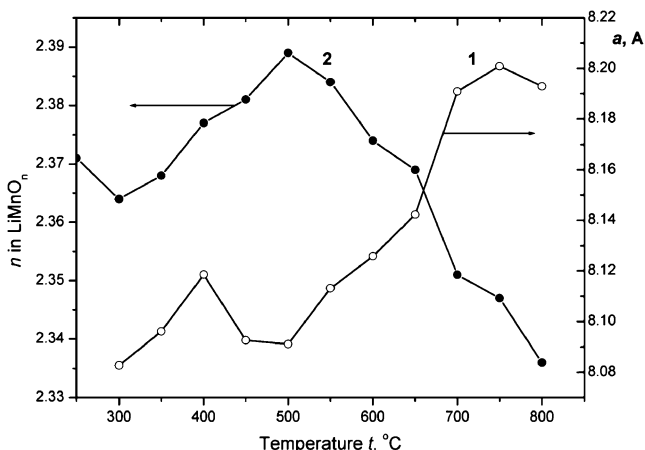


Fig. 4 Lattice parameter of the cubic cell (1) and oxygen content in the empiric formula of the sample (2) vs. the treatment temperature

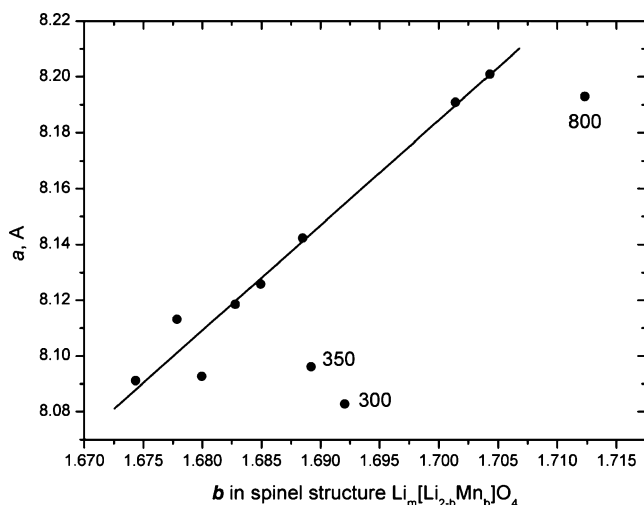
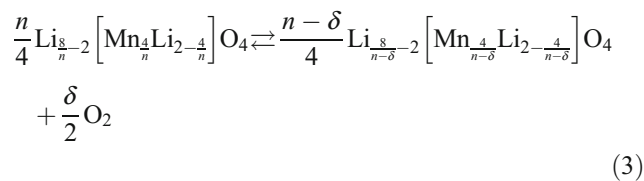


Fig. 5 Linear correlation between the lattice constant and the number of Mn atoms in the spinel formula. The decomposition temperatures (in degrees Celsius) for the three samples, which drop out of the correlation, are indicated in the figure

larger (0.645 Å in the high spin state) than the ones of Mn^{4+} (0.53 Å) and Li^+ (0.59 Å on tetrahedral coordination) [20], the lattice expands and the lattice constant increases. Such regularity is observed in the temperature region from 500 to 750 °C; the tendency is opposite at the temperatures below 500 °C. It means that the lower temperature samples are not the equilibrium ones—that is, the equilibrium 2 is not established at the temperatures 450 °C and below. Possibly, the reason for the formation of these initial phases with lower than expected oxygen content is the local overheating due to the highly exothermic character of the reaction 1.

The equilibrium 2 in the spinel notation can be written as



It means that the withdrawal of one atom of Li from the octahedral position of the whole lattice brings about the appearance of the one additional Li atom in the tetrahedral position and evolution of one oxygen molecule to the air. Schematically it can be denoted as



Assuming that the equilibrium 4 is established in the temperature range 500–750 °C and taking into account that the partial pressure of the ambient oxygen is constant, we can calculate the enthalpy of this reaction (3.9 ± 0.5 kJ) plotting the logarithm of equilibrium constant $K = \frac{[\text{Li}_{\text{tet}}]}{[\text{Li}_{\text{oct}}]}$ vs. the reverse temperature (Fig. 6).

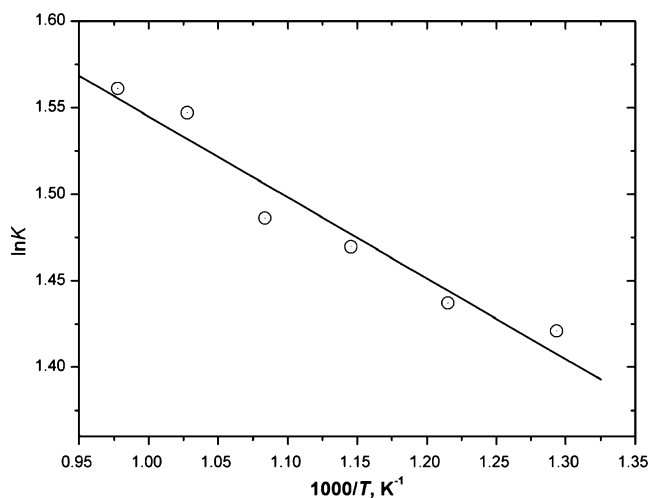


Fig. 6 Arrhenius plot for the equilibrium constant of the reaction 4

The overstoichiometric spinel phase becomes unstable at higher temperature, when n in the empiric formula LiMnO_n approaches ~ 2.33 . It decomposes forming two stable phases—normal spinel LiMn_2O_4 and manganate Li_2MnO_3 :



The reaction 5 begins at 700°C and is completed at 800°C . The data of the electrochemical investigations, which are shown in Figs. 7 and 8, are in good agreement with the proposed mechanism of the thermal decomposition.

In particular, the high-temperature sample (850°C) exhibits typical behavior of the LiMn_2O_4 stoichiometric spinel, with doubled charge and discharge peaks near 4 V on LSV curves (Fig. 7) or two plateaus on galvanostatic curves (Fig. 8). The experimental reversible capacity ($\sim 50 \text{ mAh/g}$) is lower than expected for equimolar mixture LiMn_2O_4 and Li_2MnO_3 (89 mAh/g), which can be

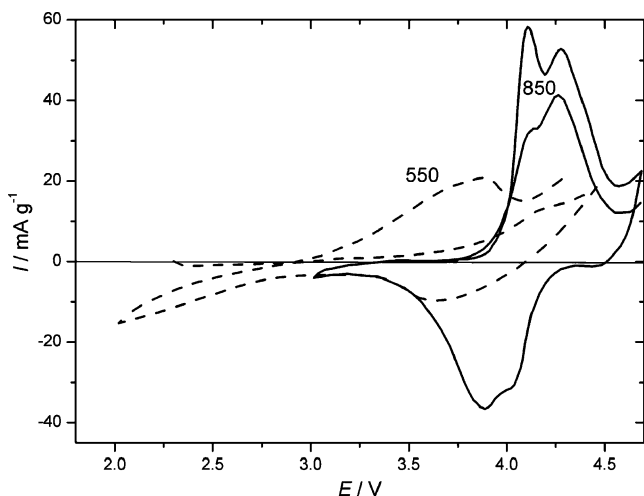


Fig. 7 Linear sweep voltammetry of the samples prepared at 850°C (solid line) and 550°C (dashed line), scan rate 0.1 mV/s

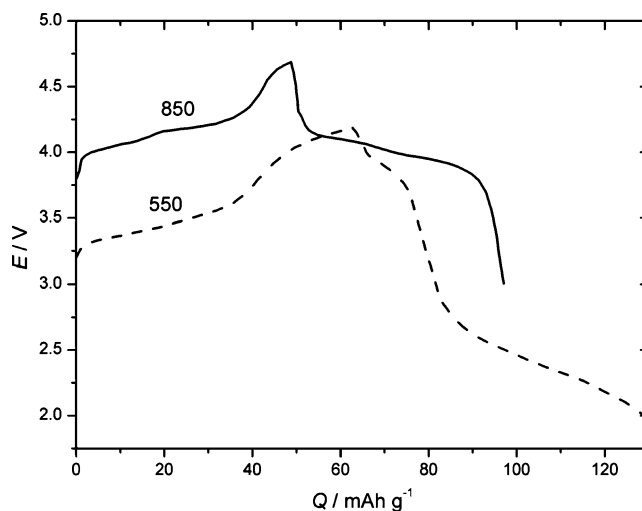


Fig. 8 Galvanostatic charge–discharge curves of the samples prepared at 850°C (solid line) and 550°C (dashed line), specific current $i=12 \text{ mA/g}$

explained by partial blocking of the spinel crystals with the electrochemically inactive manganate.

For the sample obtained at the intermediate temperature of 550°C , the current peak at approximately 3.6 V vs. Li is observed (Fig. 7, dashed line). Judging from the spinel formula of this sample given in Table 1, it corresponds to the reversible extraction of the overstoichiometric Li. Following the results of the galvanostatic cycling in the $2\text{--}4.5 \text{ V}$ range (Fig. 8), the reversible capacity of this process is $63\text{--}65 \text{ mAh/g}$, which agrees perfectly with the calculated value 62 mAh/g .

Conclusions

It was found that the final decomposition products of $\text{LiMnO}_4 \cdot 3\text{H}_2\text{O}$ is the equimolar mixture of LiMn_2O_4 and Li_2MnO_3 , which are formed at the temperatures above 700°C . Before that, at the lower temperatures, the compounds with spinel structure are formed with Li atoms being in three different states: (1) together with Mn atoms in the octahedral positions B of the spinel structure AB_2O_4 , (2) in the normal tetrahedral positions A of the structure and (3) in the excessive tetrahedral position relatively to the normal spinel. These compounds with general formula $\text{Li}_a[\text{Mn}_b\text{Li}_{(2-b)}]\text{O}_4$, which we can denote as overstoichiometric spinels, are electrochemically active with regard to the electrochemical extraction and insertion of Li in aprotic electrolytes of Li-ion cells. The specific capacities and energies of such compounds are too low for practical application as active materials of Li batteries. However, the fact that such compounds exist suggests some new approaches to the synthesis of Mn-based electrochemically active oxide materials. For example, there is an interesting possibility to replace the

octahedral Li atoms with the atoms of other transition metals. This possibility is worthwhile to be studied in future.

Acknowledgments This work was supported in part by Ministry of Science and Education of Ukraine, project #2991F, and Spanish MICINN (MAT2010-15094 and MAT2006-01997).

References

1. Linden D, Reddy TB (2002) Handbook of batteries, 3rd edn. McGraw-Hill, New York
2. Du Pasquier A, Blyr A, Courjal P, Larcher D, Amatucci G, Gerard R, Tarascon J-M (1999) *J Electrochem Soc* 146:428–436
3. Prisiazhnyi VD, Andriiko AA, Chmilenko NA (2001) *Elektrokhimicheskaya Energetika* 1:73–79, in Russian
4. Nohma T, Saito T, Furukawa N, Ikeda H (1989) *J Power Sources* 26:389–396
5. Nohma T, Yamamoto Y, Nakane I, Furukawa N (1992) *J Power Sources* 39:51
6. Andriiko A, Nyrkova LI, Chmilenko NA, Rudenok PV, Kuzminskii EV (1996) *Solid State Ionics* 86–88:805–809
7. Reimers JN, Fuller EW, Rossen E, Dahn JR (1993) *J Electrochem Soc* 140:3396–3401
8. Koetschau I, Richard MN, Dahn JR, Soupart JB, Rousche JC (1995) *J Electrochem Soc* 142:2906–2910
9. Crouguennec L, Deniard P, Brec R (1997) *J Electrochem Soc* 144:3323–3330
10. Myung ST, Komaba S, Kumagai N (2001) *Chem Lett* 1:80
11. Thackeray MM, David WIF, Bruce PG, Goodenough JB (1983) *Mater Res Bull* 18:461–472
12. Tarascon J-M, Guyomard D (1991) *J Electrochem Soc* 138:2864–2868
13. Tarascon J-M, Wang E, Shokoohi F, McKinnon WR, Colson S (1991) *J Electrochem Soc* 138:2859–2864
14. Gummow RJ, De Kock A, Thackeray MM (1994) *Solid State Ionics* 69:59–67
15. Abiko H, Hibino M, Kudo T (2000) Extended abstracts. Symposium on Solid State Ionics in Japan 26:16–17
16. Dong HJ, Seung MO (1997) *J Electrochem Soc* 144:3342–3348
17. Thackeray M, De Kock A, Rossow MN, Liles D, Bittihn R, Hoge D (1992) *J Electrochem Soc* 139:363–366
18. Meyer G, Hoppe R (1976) *Z Anorg Allgem Chem* 424:257–264
19. Shao-Horn Y, Ein-Eli Y, Robertson AD, Averill WE, Hackhey SA, Howard WF (1998) *J Electrochem Soc* 145:16–23
20. Shannon RD (1976) *Acta Cryst* A32:751–767